

# Seasonal study of calcite-water oxygen isotope fractionation at recent freshwater tufa sites in Hungary

BARBARA BÓDAI<sup>1,✉</sup>, GYÖRGY CZUPPON<sup>2,3</sup>, ISTVÁN FÓRIZS<sup>2,3</sup> and SÁNDOR KELE<sup>2,3</sup>

<sup>1</sup>Eötvös Loránd University, Institute of Geography and Earth Sciences. Department of Physical Geography, 1117 Budapest, Hungary; ✉[bodai.barbara@gmail.com](mailto:bodai.barbara@gmail.com)

<sup>2</sup>Institute for Geological and Geochemical Research, Research Centre for Astronomy and Earth Sciences, ELKH, Budapest, Budaörsi út 45, 1112 Hungary; [kele.sandor@csfk.org](mailto:kele.sandor@csfk.org)

<sup>3</sup>CSFK, MTA Centre of Excellence, Budapest, Konkoly Thege Miklós út 15–17, 1121 Hungary

(Manuscript received November 3, 2021; accepted in revised form August 5, 2022; Associate Editor: Michal Šujan)

**Abstract:** Recent fluvial tufa carbonates were investigated from the Szalajka Valley (Bükk Mts., Hungary) and Malom Valley (Balaton Uplands, Hungary) to (1) study the suitability of the published oxygen isotope-based palaeothermometers for tufa deposits, (2) find the most appropriate (closest to equilibrium) places downstream for temperature calculation. A good correlation was observed between  $1000\ln\alpha$  and the temperature of the water from which the tufa precipitated close to the spring orifice in the Szalajka and Malom Valleys. Large differences between calculated and measured temperature values were seen in areas where the seasonal water temperature increased and decreased by several degrees during our studied period. The stable isotope composition of the measured Hungarian tufas represents intermediate values between the western and eastern parts of Europe, reflecting increasing continentality in climate from west to east.

**Keywords:** freshwater tufa, stable carbon and oxygen isotopes, geochemistry, palaeothermometry, Hungary

## Introduction

Freshwater tufas are continental carbonate sediments formed under open-air conditions from ambient, primarily cool temperature (karst) waters in areas of carbonate bedrock (Pentecost 2005; Capezzuoli et al. 2014). Their precipitation is strongly influenced by changes in supersaturated water dynamics, leading to intense physicochemical and/or biological process of  $\text{CO}_2$  degassing in the hydrological regime.

Freshwater carbonates (tufa) are studied worldwide, as their formation is related to environmental parameters and can therefore be widely used as an indicator of past climate (see e.g. Pazdur 1988; Andrews & Brasier 2005; Andrews 2006; Dabkowski 2014; Garnett et al. 2014; Dabkowski et al. 2015, 2019; Berrendero et al. 2016). The temperature dependence of calcite-water oxygen isotope composition is used to calculate the temperature of carbonate depositions (e.g. Matsuoka et al. 2001; Osácar et al. 2013; Kele et al. 2015). Additionally, the clumped isotope thermometer, which does not require knowledge of the oxygen isotope composition of water, may also be used to calculate the temperature of carbonate depositions (Kim & O'Neil 1997; Ghosh et al. 2006; Eiler 2007; Tremaine et al. 2011; Kele et al. 2015; Kele & Bajnai 2017). The temperature of the water can be calculated (only in the case of equilibrium) with calcite-water oxygen isotope fractionation equations that incorporate the oxygen isotope composition of freshwater carbonates and their depositing water. Urey (1947) created the first equation for the calculation of palaeotemperature, based on inorganic and biogenic carbonates. Epstein et al. (1951) followed, demonstrating

the temperature dependence of oxygen isotope fractionation between water and calcite. Epstein et al. (1953) developed the first practical oxygen isotope temperature scale, based on the oxygen isotopic composition of biogenic carbonates. Over time, several new equations (e.g. Friedman & O'Neil 1977; Kim & O'Neil 1997; Tremaine et al. 2011; Kele et al. 2015) were created to calculate the precipitation temperature of carbonates in different depositional environments and temperature ranges. Most of these equations, however, were not specifically designed for tufa carbonates. To increase the accuracy of these calculations, it is necessary to understand the isotope fractionation processes between the carbonate and water phases, in which the study of recently forming tufas may help. In our calculations, we used the equations in Kim & O'Neil (1997), Tremaine et al. (2011), and Kele et al. (2015). The equation (1) in Kim & O'Neil (1997) is based on a synthetic calcite experiment with a relatively narrow temperature range (10–40 °C) that partly overlaps with the values measured in this study.

$$1000\ln\alpha = 18.03 * 1000/T - 32.42 \quad (1)$$

The Tremaine et al. (2011) equation (2) was developed based on cave carbonates, where the cave system is relatively closed and the rate of precipitation is continuous with a balanced temperature.

$$1000\ln\alpha = 16.1 * (1000/T) - 24.6 \quad (2)$$

The Kele et al. (2015) equation (3) (6–95 °C) is used because it is based on several different carbonates, including travertine, freshwater tufa and biogenic carbonates.

$$1000\ln\alpha = (16.8 \pm 1.7) * 1000/T - (26 \pm 5.4) \quad (3)$$

Actively forming freshwater tufa carbonates and concomitant water samples were taken from the Szalajka (Bükk Mts., Hungary) and Malom (Balaton Upland, Hungary) streams as well. We also compared the stable isotope values of tufas, measured in the stream, to the stable isotope data of tufas from other Hungarian mountains, as well as to the values from neighbouring countries (Andrews 2006). This was important because it helped us to understand the reason for regional differences and/or similarities in the stable isotope composition of tufas, which is crucial for their palaeoenvironmental and palaeoclimatic interpretation.

Several recently forming freshwater tufa deposits are found in the Bükk Mts. (Fig 1A) (Hevesi 1972). On their northern side, water-bearing rocks overlie the Palaeozoic formations, whereas on their southern side, towards the Great Hungarian Plain, the water-bearing rocks extend deep and are covered by Neogene and Quaternary sediments (Aujeszky et al. 1974; Aujeszky & Scheuer 1979). The multilevel karst system evolved in the Bükk Mountain Range, due to the different hydraulic conductivity of the rocks (Aujeszky et al. 1974; Aujeszky & Scheuer 1974). The springs on the northern side

of the Bükk Mts. discharge at relatively high altitude and are characterised by significantly variable discharge and low temperature. Additionally, their aquifer is primarily composed of Carboniferous–Permian and upper Eocene limestone. The climate of the northern part of the Bükk Mts. is continental, with seasonal contrasts in temperature. The mean annual air temperature and precipitation amount are  $\sim 10^\circ\text{C}$  and  $\sim 860$  mm, respectively (OMSZ 2001).

The Szalajka Valley is near the village of Szilvásvár (Bükk Mts., NE Hungary) (Table 1; Fig. 1B). The Szalajka stream cuts into this valley (Zsilák 1960). On the upper part of the Szalajka Valley, there are many freshwater tufas whose thickness is largely unknown. The freshwater tufa deposits are primarily linked to morphological steps (i.e., cascades, rapids, dams), where the turbulence and related  $\text{CO}_2$  degassing are intense, and the tufa forms in the barrage/dam perpendicular to the flow direction. There are several fishponds, pools and small lakes along the Szalajka Valley, and their water flows into the Szalajka stream in a SE to NW direction. The Szalajka Spring (Figs. 1B, 2A), with a mean annual discharge of  $\sim 4500$  L/min, is the main source of the Szalajka stream (Pelikán 2005). Its catchment area is the karstic Bükk Plateau ( $8\text{--}10$  km<sup>2</sup>). The Szalajka Spring discharges at an altitude of

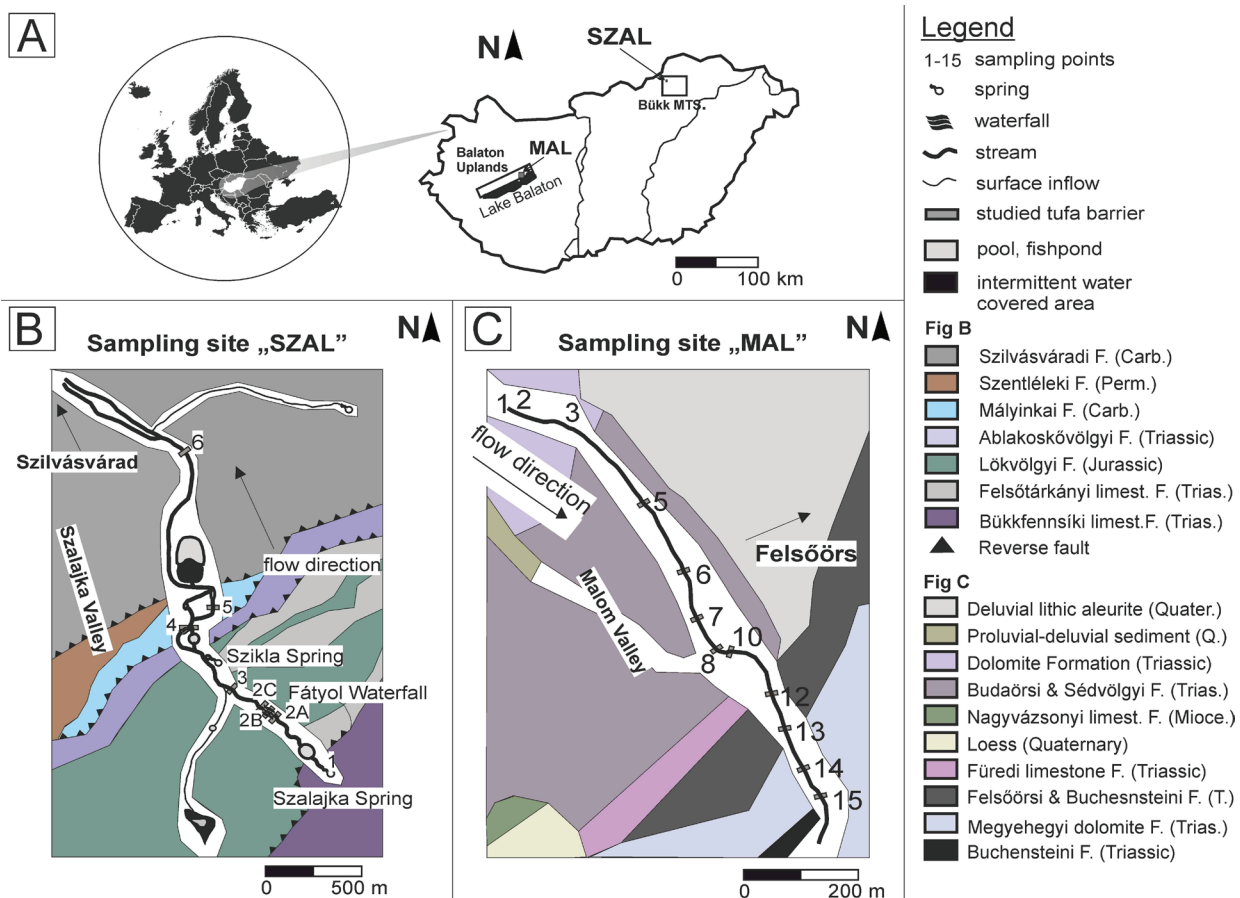


**Fig. 1.** A — The location of the study sites in Hungary. B — Map of the tufa-bearing stream in the Szalajka Valley, Bükk Mts. C — Map of the tufa-bearing stream in the Malom Valley, Balaton Uplands. The (B) and (C) maps are supplemented by geological settings ([www.map.mbfisz.gov.hu](http://www.map.mbfisz.gov.hu)).

**Table 1:** The location and coordinates of the sampling points, indicating downstream distances from the spring orifices (Szalajka Valley, Bükk Mts. and Malom Valley, Balaton Uplands).

Location	Code	Distance from the spring (km)	Coordinates	
Bükk, Szalajka V.	SZAL-1	–	N48°04'22.26"	E20°24'54.27"
Bükk, Szalajka V.	SZAL-2A	0.450	N48°04'33.07"	E20°24'41.17"
Bükk, Szalajka V.	SZAL-2B	0.462	N48°04'33.74"	E20°24'36.59"
Bükk, Szalajka V.	SZAL-2C	0.530	N48°04'34.51"	E20°24'34.44"
Bükk, Szalajka V.	SZAL-3	0.704	N48°04'35.61"	E20°24'31.52"
Bükk, Szalajka V.	SZAL-4	0.997	N48°04'46.55"	E20°24'20.45"
Bükk, Szalajka V.	SZAL-5	1.126	N48°04'50.08"	E20°24'37.26"
Bükk, Szalajka V.	SZAL-6	2.056	N48°05'22.42"	E20°24'13.07"
Balaton Uplands, Malom V.	MAL-1	–	N47°01'03.59"	E17°56'23.33"
Balaton Uplands, Malom V.	MAL-2	0.002	N47°01'03.59"	E17°56'23.33"
Balaton Uplands, Malom V.	MAL-3	0.082	N47°01'03.43"	E17°56'26.23"
Balaton Uplands, Malom V.	MAL-5	0.287	N47°00'59.15"	E17°56'33.18"
Balaton Uplands, Malom V.	MAL-6	0.406	N47°00'56.66"	E17°56'57.05"
Balaton Uplands, Malom V.	MAL-7	0.545	N47°00'56.66"	E17°56'57.05"
Balaton Uplands, Malom V.	MAL-8	0.590	N47°00'51.09"	E17°56'40.17"
Balaton Uplands, Malom V.	MAL-10	0.602	N47°00'52.07"	E17°56'40.48"
Balaton Uplands, Malom V.	MAL-12	0.697	N47°00'48.83"	E17°56'43.91"
Balaton Uplands, Malom V.	MAL-13	0.750	N47°00'47.09"	E17°56'45.03"
Balaton Uplands, Malom V.	MAL-14	0.816	N47°00'45.17"	E17°56'46.97"
Balaton Uplands, Malom V.	MAL-15	0.893	N47°00'43.76"	E17°56'48.89"

450 m (a.s.l.) (Hevesi 1972), and the water reaches the surface at the border of the Triassic limestone layer and impermeable clay shale (Aujeszky & Scheuer 1979). Another important source of the Szalajka stream is the Szikla Spring (Fig. 2C), which has a balanced, lukewarm water temperature of 10–12 °C. The Szikla Spring feeds primarily locally infiltrated precipitation, with a minor thermal component that is an upwelling from the deep karst system. It is located 1 km down from the Szalajka Spring (423 m a.s.l.), and the water here surfaces at the bottom of a limestone cliff (Figs. 1B, 2A). The largest amount of the water of the Szikla Spring derives from lower Triassic rocks in the NW Bükk and its drainage area is about 4–6 km<sup>2</sup> (Baráz 2002). Tracer studies show that it receives small amounts of water from the Great Plateau as well. Its mean annual discharge is ~1700 L/min but depends on the amount of precipitation. At the depression near the Szikla spring, the soil boreholes in the soil did not reach the bottom of the freshwater tufa at a depth of 8 m. Downstream, a leakage of 8500 L/min was measured around the lakes, of which 5000 L/min was returned near Measuring Point 6 (Zsilák 1960). For the Szalajka Valley, the isotopic composition of water and tufa was interpreted up to the SZAL-3 sampling point (preceding the Szikla Spring), because farther down in the sampled section, there are several surface inflows with different water temperatures and origins (e.g., Szikla Spring, fishponds), as well as the groundwater leakage and its repeated inflow into the stream.

The Balaton Uplands is a west-east elevation on the northern shore of Lake Balaton between the Bakony Mts. and the Keszthely Plateau. The eastern part is a plateau composed predominantly of Permian and Triassic sediments that rises 150–200 m above Lake Balaton (Budai et al. 1999). The highlands exceeding 300 m high are composed of cherty limestone,

which is resistant to erosion. The structural depressions of the Balaton plateau are typically filled with younger soft layers, some of which have been removed by erosion.

The Malom Valley is located at the western border of Felsőörs (Table 1; Fig. 1C), near Lake Balaton, in the pediment area of the Bakony Mts. It mainly consists of Triassic and Jurassic limestone, dolomite and less marl, which was uplifted along the faults during the Neogene (Budai et al. 1999). Because the area is composed of karstic rock, many surface and deep karst forms can be found there. The basement of the Balaton Uplands was also formed by karstic rocks, which are covered by Pannonian sediments and debris of polycyclic-monogenetic basalt volcanoes of the Pliocene–Pleistocene age. The riverbed of the Malom stream cuts into a covered karst area, and its water is derived from the karst system. Eighteen wells supply drinking water in the area.

### Meteorological data of studied sites

The nearest meteorological station to the Szalajka Valley, with monthly resolution data, is Miskolc (131 m a.s.l.), which is 28 km away. The amount of annual precipitation changed between 691 and 747 mm, and the mean air temperature changed between 10.8–11.8 °C, with the extremes exceeding 30 °C in the summer (31.1–38.1 °C in May–September, with one exception: 26.8 °C in May 2019) and 0 °C in the winter (–0.4 to –17.9 °C in October–March, with one exception: 0.9 °C in October 2018) during the measured period (from February 2016 to September 2019) ([www.ksh.hu](http://www.ksh.hu)<sup>1,3</sup>). Monthly resolution data is not available for 2016.

The nearest meteorological station to the Malom Valley is Siófok (124 m a.s.l.), which is 15 km away. The amount of



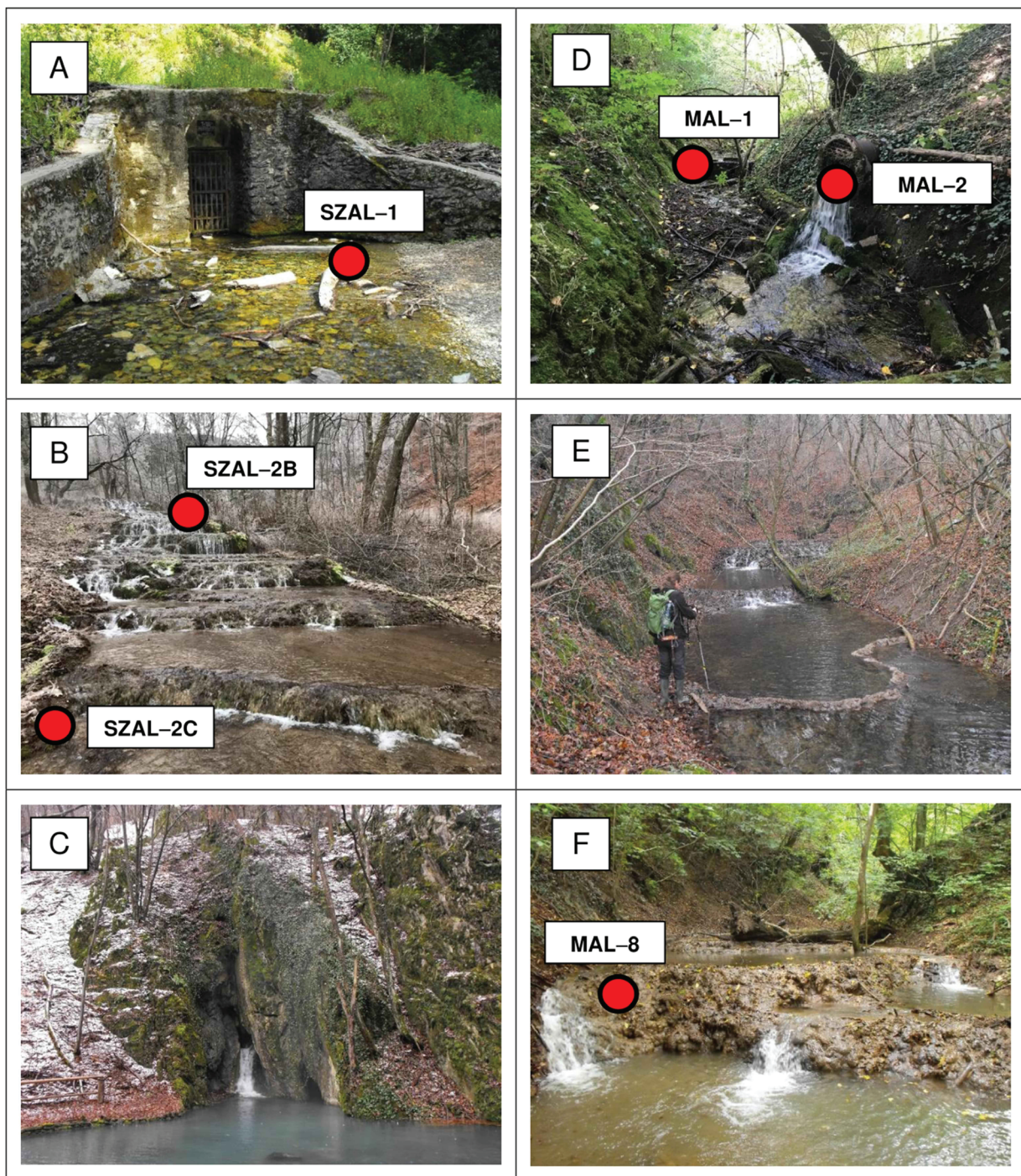


**Fig. 2.** Field photos of tufa deposits from karstic streams at the studied sites. Szalajka Valley: **A** — Sampling point 1 (SZAL-1), the Szalajka Spring orifice; **B** — The most spectacular waterfall (Fátyol Waterfall) in Hungary with its tufa barrages; **C** — The Szikla Spring. Malom Valley: **D** — Malom stream spring orifice, sampling points 1 and 2 (MAL-1 and MAL-2 are considered to be the main water source of the spring, artificial construction); **E** — Freshwater tufa dams in the Malom stream; **F** — Sampling point 8 (MAL-8), representing one of the tufa dams.

annual precipitation changed between 553 and 628 mm, and the mean air temperature changed between 12.1–13.1 °C, with the extremes exceeding 30 °C in the summer (31.5–38.0 °C, June–August) and 0 °C in the winter (–2.9 to –13.1 °C, December–February) during the measured period (from November 2017 to September 2019) ([www.ksh.hu](http://www.ksh.hu)<sup>2,3</sup>).

## Methods

### *Field measurements and sampling*

Seasonal measurements and samplings were done along the Szalajka stream in 2016 and 2019. Eight sampling points



were selected downstream at the major tufa barrages/dams along a 2.5 km long section starting from the Szalajka Spring (Table 1; Fig. 1B). We also performed seasonal monitoring measurements and sample collection along the Malom stream in 2018 and 2019, during which a total of 12 sampling points were defined along the 800 m long section (Fig. 1C). At all points, water temperature, pH and conductivity were measured *in situ*, and tufa and water samples were collected for stable isotope analyses. A Hanna HI98108 instrument (accuracy:  $T = \pm 0.5^\circ\text{C}$ ,  $\text{pH} = \pm 0.1$ ) was used to measure water temperature and pH. Conductivity (EC) was determined with a Hanna HI98303 Dist3 pen (precision:  $\pm 0.2\%$  of the total scale). Water samples were collected from both sites at the sampling points in 50 ml HDPE plastic bottles and were refrigerated until the analyses to avoid evaporation and fractionation. Tufas were sampled at 7 sampling points in the Szalajka Valley. At the first sampling point (SZAL-1), there was no tufa deposition. In the Malom Valley, tufa samples were collected at 9 stations, starting from the sampling point 5 (MAL-5) (Table 1; Fig. 2D,E,F). At the MAL-1 sampling point, the water flow rate was very low, thus, MAL-2 was the main sampling point for the Malom stream, MAL-2 also contributes the bulk of the water in the riverbed. To collect fresh carbonate, plastic surfaces were placed in the streambed and were replaced seasonally. The first sampling campaign was an exception because only the uppermost surface of the recent tufa barrages was sampled to ensure the collection of freshly precipitated carbonates.

### Stable isotope analyses

The stable carbon- and oxygen isotopic compositions ( $\delta^{13}\text{C}_c$ ,  $\delta^{18}\text{O}_c$ ) of the tufa, as well as the oxygen and hydrogen isotopic compositions ( $\delta^{18}\text{O}_w$ ,  $\delta\text{D}$ ) of the water samples, were determined at the stable isotope laboratory of the Institute for Geological and Geochemical Research (Budapest, Hungary). For carbonates, a Finnigan delta Plus XP mass spectrometer was used, following the method in Spötl & Vennemann (2003). Samples were dried overnight in an oven at  $60^\circ\text{C}$ , after which they were finely powdered and aliquots of 20–250  $\mu\text{g}$  were used for each measurement. Primarily three in house laboratory standards ( $\delta^{13}\text{C}_{\text{PDB}} = +2.05\%$ ,  $-25.80\%$ ,  $-5.74\%$ ;  $\delta^{18}\text{O}_{\text{PDB}} = -2.07\%$ ,  $-17.23\%$ ,  $-22.96\%$  for Carrara, Merck and Sp 96/4, respectively) were used for calibration purposes, with NBS-19 and NBS-18 serving as additional standard. Two-point linear normalization was applied according to Paul et al. (2007). The  $\delta^{13}\text{C}_c$  and  $\delta^{18}\text{O}_c$  values of the carbonates are reported in ‰ notation and are expressed relative to Vienna Pee Dee Belemnite (V-PDB). The  $\delta^{18}\text{O}_c$  values are also expressed relative to Vienna Standard Mean Ocean Water (V-SMOW) because the equations for temperature calculation express  $\delta^{18}\text{O}_c$  in V-SMOW. The uncertainty of data was better than  $\pm 0.1\%$  for both the  $\delta^{13}\text{C}_c$  and the  $\delta^{18}\text{O}_c$  (V-PDB) based on repeated measurements and the standard deviation of the three in house standards.

The water samples were analysed using a LGR LWIA-24d laser spectroscope. Three in house laboratory water standards were utilised for calibration ( $\delta\text{D} = -9.0\%$ ;  $-74.9\%$ ;  $-147.7\%$ ;  $\delta^{18}\text{O} = -0.53\%$ ;  $-10.41\%$ ;  $-19.95\%$  for BWS1, BWS2, BWS3 respectively), where BWS1 and BWS3 were used for the two-point normalization (Paul et al. 2007) and BWS2 was used. The  $\delta^{18}\text{O}_w$  and  $\delta\text{D}$  values of the water samples are reported relative to V-SMOW. The uncertainties of measurements were better than  $\pm 0.1\%$  and  $\pm 1\%$  for  $\delta^{18}\text{O}_w$  and  $\delta\text{D}$ , respectively. Further details can be found in Czuppon et al. (2018).

## Results

### Field observations

#### *Szalajka Valley*

Seasonal changes in water temperature were recognised along the Szalajka stream, whereas the water temperature of the Szalajka Spring (SZAL-1) remained nearly stable ( $8.5\text{--}9.4^\circ\text{C}$ ) during the studied period (2016–2019) (Supplementary Table S1; Fig. 3A). Based on 797 measurements (www.bnpi.hu), the water discharge between 1940 and 1999 varied from 138 to 37,800 L/min, and small amounts of groundwater 1–2 months old were potentially mixed. The meteorological data indicate that the cool (October to March) and warm (April to September) seasons can be differentiated. During cool seasons, the temperature of the stream decreased downstream, whereas, during warm seasons, it increased (Suppl. Table S1). Up to the SZAL-4 sampling point, the constantly lukewarm water ( $10\text{--}12^\circ\text{C}$ , Baráz 2002) of Szikla Spring mixes with the water of the Szalajka stream, changing its temperature. The lowest ( $1.4^\circ\text{C}$ , December 2018) and the highest ( $15.4^\circ\text{C}$ , September 2019) temperatures were measured at the SZAL-3 sampling point (Fig. 3A). The Szalajka stream is located in a wide ( $10\text{--}100\text{ m}$ ) valley bottom, where the movement of air is less restricted, and environmental factors may have a greater effect on its water temperature compared to the Malom Valley.

The pH values increased downstream during the studied periods (Suppl. Table S1; Fig. 3B). The total change in pH along the longitudinal profile is about  $0.7\text{--}1.7$  pH units, and the lowest pH values (between 6.47 and 7.82) were observed each time at the Szalajka spring, where freshwater tufa precipitation was not found (Suppl. Table S1; Fig. 3B).

The EC values decrease up to Sampling Point 3 (exception: September 2019, SZAL-2A). At SZAL-4, where the Szikla Spring inflows, the EC values are higher than the values at SZAL-3 (exception: August 2016, SZAL-4, where it was the lowest value in that period) (Suppl. Table S1).

#### *Malom Valley*

At the main source of the Malom stream (MAL-2 sampling point), the water temperature ranged from  $11.2$  to  $12.3^\circ\text{C}$

(Suppl. Table S2; Fig. 4A) and did not show significant seasonal changes. The water temperature increased downstream during warm periods and decreased during cold periods, but in each case the change was less than 2.1 °C. In spring and autumn (October 2018, March 2019, and September 2019), the water temperatures did not change significantly downstream ( $\pm 1$  °C). Both the warmest (14.7 °C) and the coldest (8.3 °C) temperatures were measured at the downstream end of the section (Suppl. Table S2; Fig. 4A). The Malom stream is located in a narrow, shady and approximately V-shaped valley 3–10 m wide with steep slopes. The temperature of the water samples varied between 12.5–14.7 °C during warm periods and 8.3–11.6 °C during cold periods. The total change in the downstream water temperature during each measuring period was approximately  $\pm 2$  °C, but the Malom stream is 800 m shorter than the Szalajka Stream.

The pH values increased downstream from MAL-3 (Suppl. Table S2; Fig. 4B). The pH ranged between 7.34 and 8.48 (November 2017); 7.15 and 8.32 (May 2018); 7.13 and 8.51 (October 2018); 7.38 and 8.56 (March 2019); 7.34 and 8.25 (June 2019); 7.41 and 8.42 (September 2019).

The EC values showed a downstream decrease (Suppl. Table S2) and ranged between 924 and 775  $\mu\text{S}/\text{cm}$  (exception: 496, November 2017).

### Isotopic composition of water

The  $\delta^{18}\text{O}_w$  of the Szalajka stream water varied between  $-10.6$  and  $-10.0$  ‰ (V-SMOW) (Suppl. Table S1). The  $\delta\text{D}$  values ranged from  $-72$  ‰ to  $-69$  ‰ (V-SMOW), showing similar trends to the  $\delta^{18}\text{O}_w$  (Suppl. Table S1). The change in the isotope composition ( $\delta^{18}\text{O}$ ,  $\delta\text{D}$ ) of the water is close to the uncertainty of the analyses.

In the case of the Malom Valley, the  $\delta^{18}\text{O}_w$  and  $\delta\text{D}$  values of water did not show seasonal or downstream changes along the studied section, or, they are within the analytical error. The  $\delta^{18}\text{O}_w$  varied between  $-9.9$  and  $-9.4$  ‰ V-SMOW, while the  $\delta\text{D}$  ranged from  $-70$  to  $-67$  ‰ V-SMOW (Suppl. Table S2).

### Isotopic composition of tufa

The stable isotope values of the freshwater tufas of the Szalajka and Malom streams are summarised in Suppl. Tables S1 and S2. The  $\delta^{13}\text{C}_c$  and  $\delta^{18}\text{O}_c$  values of the Szalajka samples are similar to other published tufa isotope values from the Bakony and Mecsek Mts. (Kele 2009; Koltai et al. 2012a,b; Bódaï et al. 2015, 2016), as well as to the values from neighbouring countries (Andrews 2006) (Fig. 5A). The stable isotope compositions of the measured Hungarian tufas represent intermediate values between Western and Eastern Europe,

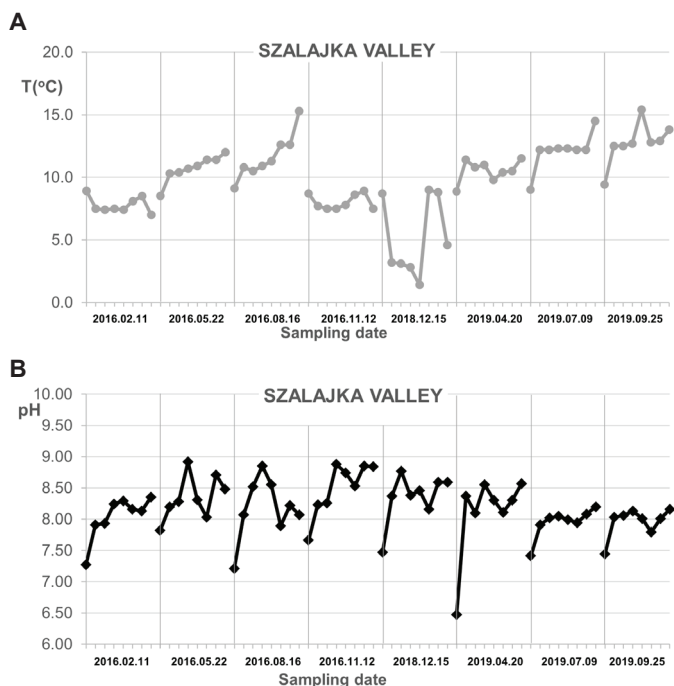


**Fig. 3.** A — Seasonal pattern of water temperature for all the sampling points in the Szalajka stream – sampling points in increasing order within one date. Data were collected seasonally in 2016, at the end of 2018 and in 2019. B — Seasonal pattern pH for all the sampling points in the Szalajka stream – sampling points in increasing order within one date. Data were collected seasonally in 2016, at the end of 2018 and in 2019.

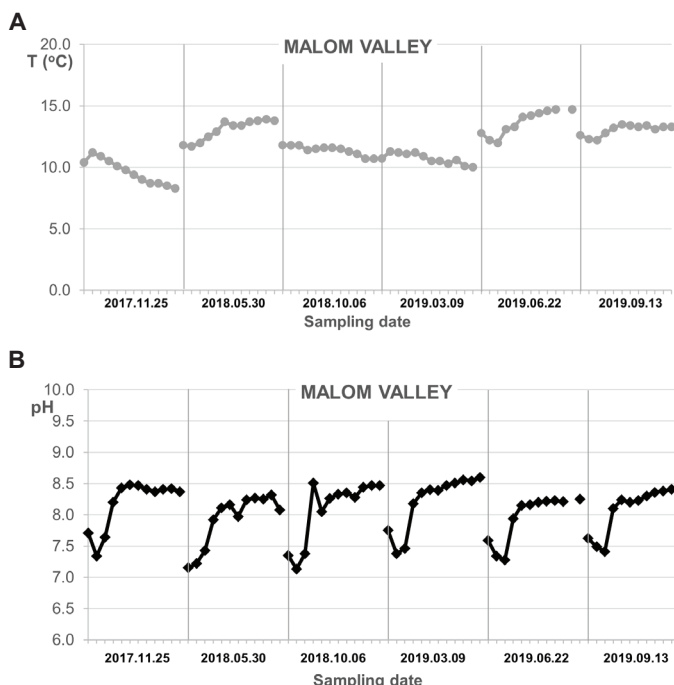


**Fig. 4.** A — Seasonal pattern of water temperature for all the sampling points in the Malom stream – sampling points in increasing order within one date. Data were collected seasonally at the end of 2017, 2018 and 2019. B — Seasonal pattern of pH for all the sampling points in the Malom stream – sampling points in increasing order within one date. Data were collected seasonally at the end of 2017, 2018 and 2019.



reflecting increasing continentality in climate from west to east, as was observed by Andrews (2006).

The  $\delta^{18}\text{O}_c$  varied between  $-10.1$  and  $-7.9$  ‰ V-PDB in the Szalajka Valley and between  $-9.0$  and  $-8.0$  ‰ V-PDB in the Malom Valley. The  $\delta^{13}\text{C}_c$  of the Szalajka Valley varied between  $-10.8$  and  $-7.9$  ‰ V-PDB, whereas the Malom Valley's  $\delta^{13}\text{C}_c$  varied between  $-10.5$  and  $-9.1$  ‰ V-PDB (Suppl. Tables S1 and S2). The  $\delta^{13}\text{C}_c$  and  $\delta^{18}\text{O}_c$  values of the Szalajka and Malom Valleys' freshwater tufa showed significant overlap during the studied periods (Fig. 5A, B and Figs. 6, 7).

The  $\delta^{18}\text{O}_c$  values of the Szalajka Valley showed more positive changes downstream between the first (SZAL-2B in 2016 and SZAL-2A in 2018/2019, 462 and 450 m away from the spring, respectively) and last measuring points (SZAL-2C/SZAL-3, 530 and 704 m away from the spring, respectively) (Fig. 6). This change is similar to the change in pH, which may be related to the Fátýol waterfall, where tufa deposition is significant (Suppl. Table S1). pH data showed the lowest values at the Szalajka Spring orifice and the highest values near the bottom of the waterfall (SZAL-3). The  $\delta^{18}\text{O}_c$  values in the Malom Valley may show smaller seasonal changes. During the summer-autumn period in October 2018 and September 2019, the decrease of  $\delta^{18}\text{O}_c$  is very weak; the seasonal changes were small during the winter-spring period in March 2019 and the  $\delta^{18}\text{O}_c$  values stagnated in November 2017, May 2018, and June 2019 (Suppl. Table S2; Fig. 7).

Seasonal changes can be observed in the  $\delta^{13}\text{C}_c$  of the Szalajka Valley (Suppl. Table S1). The data from the winter-spring periods show a decrease downstream (in February 2016, May 2016, and April 2019) but an increase downstream during the summer-autumn periods (in August 2018, November 2016, December 2018, July 2019, and September 2019).

The  $\delta^{13}\text{C}_c$  values in the Malom Valley decreased downstream up to the MAL-12 sampling point, and then increased in November 2017, May 2018 and October 2018 (Suppl. Table S2). In March 2019, the  $\delta^{13}\text{C}_c$  values were stable, before they increased in June 2019 and September 2019.

### Oxygen isotope fractionation between tufa carbonate and water

The oxygen isotope fractionation between tufa carbonate and water is temperature-dependent (Urey 1947; McCrea 1950). In the case of equilibrium, the  $\delta^{18}\text{O}_c$  is controlled primarily by the  $\delta^{18}\text{O}$  value of the depositing water and the temperature of deposition. The fractionation factor ( $\alpha$ ) can be calculated from the measured  $\delta^{18}\text{O}_w$  and  $\delta^{18}\text{O}_c$ . In our case, the  $\alpha$  is mainly determined by the water temperature, as the  $\delta^{18}\text{O}$  values of the water may be considered nearly constant at both studied sites.

The covariance of the depositing temperature and all  $1000\ln\alpha$  values calculated from the Szalajka Valley freshwater tufa is  $r=0.2065$  (p-value: 0.3223, n: 25) for the studied period. The  $1000\ln\alpha$  values are only slightly different for warm ( $r=0.1411$ , p-value: 0.5891, n: 17) and cool ( $r=0.1688$ , p-value: 0.3120, n: 8) periods.

To select the most suitable points for temperature calculation (Suppl. Table S3), the calculated  $1000\ln\alpha$  values were compared based on the distance from the spring and the temperature change at the given measuring point. In the case of the Szalajka Valley, based on the p-value, the SZAL-2B sampling point (462 m away from the spring) provides the best covariance ( $r=0.8329$ , p-value: 0.0102, n: 8,  $\Delta T=9.4$  °C).

In the case of the Malom Valley, the covariance between all calculated  $1000\ln\alpha$  values and depositing temperatures is  $r=0.2025$  (p-value: 0.1674, n: 48) for the study period, with  $r=0.5251$  (p-value: 0.0120, n: 22) for the warm periods and  $r=0.0271$  (p-value: 0.8950, n: 26) for the cold periods. This suggests that the covariance between the calculated  $1000\ln\alpha$  and the warm periods is good, whereas, between the calculated  $1000\ln\alpha$  and the cold periods, the covariance is negligible.

The strongest correlation ( $r=0.8147$ , 406 m away from the spring, p-value: 0.0483, n: 6,  $\Delta T=3.2$  °C) was found at sampling point MAL-6. At other measuring points the covariance was negligible (Suppl. Table S3). The  $N=6$  is less than the minimum required number of elements ( $N=8$ ) (Jenkins &

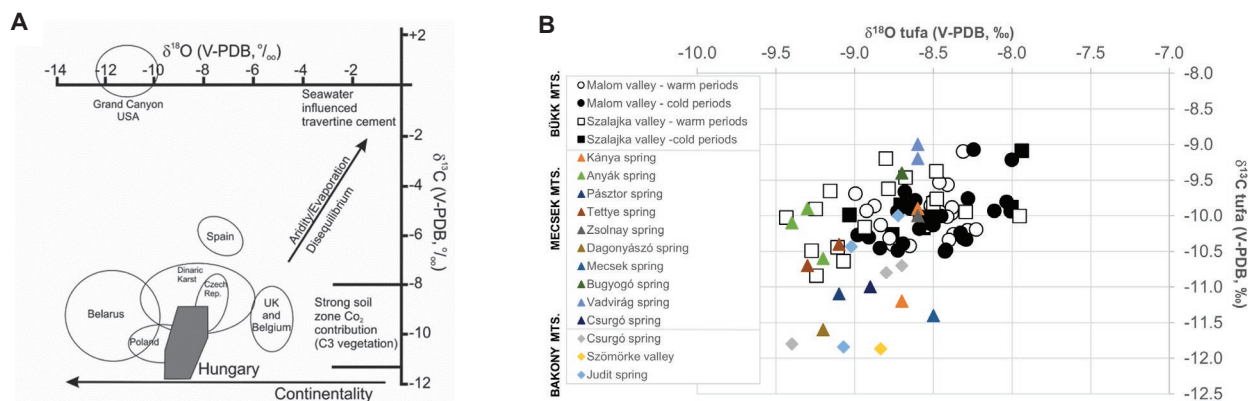


**Fig. 5. A** — Comparison of the stable isotopic composition of recent tufa sites in Hungary with those of neighbouring countries, established by Andrews (2006). **B** — Seasonal variation of Szalajka and Malom Valley tufa  $\delta^{13}\text{C}$  and  $\delta^{18}\text{O}$  values compared with  $\delta^{13}\text{C}$  and  $\delta^{18}\text{O}$  values of other Hungarian tufas.

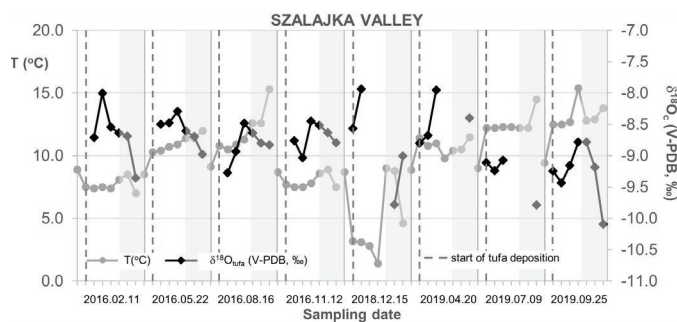


**Fig. 6.** Comparison of  $\delta^{18}\text{O}_e$  and pH values during the studied period in the Szalajka Valley. Sampling points in increasing order within one date.

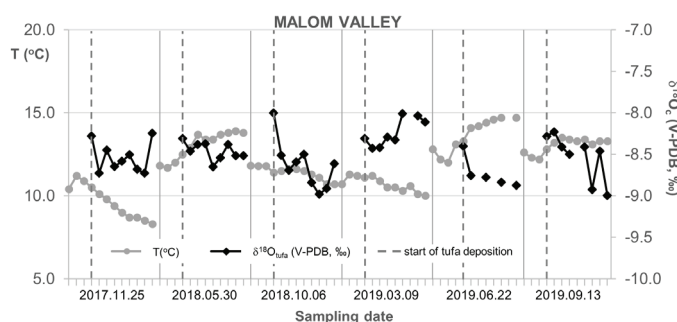


**Fig. 7.** Comparison of  $\delta^{18}\text{O}_e$  and pH values during the studied period in the Malom Valley. Sampling points in increasing order within one date.

Quintana-Ascencio 2020), so the conclusion is uncertain and needs later improvement.

The calculated  $1000\ln\alpha$  values for both sites were compared with previously published regressions lines (Fig. 8), and the calculated  $1000\ln\alpha$  values were fit to the equations in Kim & O'Neil (1997), and Tremaine et al. (2011).

## Discussion

### Stable isotope composition of tufa and water

The temperature change of the springs in the Szalajka and Malom Valleys was approximately  $1^\circ\text{C}$ , and the  $\delta^{18}\text{O}_w$  values are considered to be nearly constant. At the orifice of the springs at both of the studied sites, the  $\delta^{18}\text{O}$  and  $\delta\text{D}$  values were relatively constant during the measuring time, suggesting that the residence time and/or different subsurface inflow may have influenced the  $\delta^{18}\text{O}_w$  values (Matsuoka et al. 2001; Kano et al. 2003). The  $\delta^{18}\text{O}_w$  values at the Szalajka Spring orifice are about 1 ‰ more negative ( $-10.6$  to  $-10.4$  ‰, 450 m a.s.l.) than the values in the Malom Valley ( $-9.7$  to  $-9.5$  ‰, 210 m a.s.l.), which may be a result of the “altitude effect” (Ambach et al. 1967). Kern et al. (2020) reported altitude effects at various sites and in different seasons in the Adriatic–Pannonian region to range between 0.1 and  $-0.35$  ‰/100 m, but even the highest absolute value ( $-0.35$  ‰/100 m) cannot explain the difference of 0.9 ‰

observed in this study. Thus, in addition to the altitude effect, other factors may have played a role, as well. One possible explanation may involve the different source regions of the precipitation at the two sites. In the Bükk Mts., the ratio of precipitation originating in Northeastern Europe is higher than in the Balaton Uplands (Czuppon et al. 2017; Kern et al. 2020). Downstream, in the Szalajka Valley, the water temperature changes seasonally due to the ambient temperature.

The  $\delta^{18}\text{O}_w$  values in the Malom Valley were predominantly constant, both seasonally and downstream, and did not show a correlation with water temperature. This may be because the water discharge is more even here than in the Szalajka Valley. The  $\delta\text{D}$  water did not change, either, thus, the evaporation impact was not observed.

The  $\delta^{13}\text{C}_c$  and  $\delta^{18}\text{O}_c$  values of the Szalajka and Malom Valleys are very similar to each other (Fig. 5A, B), which may be similarities in the plant and soil activity that provides organic  $\text{CO}_2$  with low  $\delta^{13}\text{C}$ . The summer downstream decrease and the winter downstream increase may be due to changes in water temperature. It should be noted that the mean annual air temperature was similar to the spring's water temperature (measured at the MAL-2 sampling point) during the measuring period, which may have resulted in small water temperature fluctuations.

### Temperature estimations

At the sampling points SZAL-2B (located 462 m distance from the Szalajka Valley spring) and MAL-6 (406 m distance from the Malom Valley spring), we found a good correlation between tufa depositing temperatures and  $1000\ln\alpha$  values. This may suggest that they are the ideal locations to calculate tufa depositing temperatures. To calculate the deposition temperature of recent tufa, we used the equations in Kim & O'Neil (1997), Tremaine et al. (2011) and Kele et al. (2015) (which includes tufa samples from the Szalajka Valley, as well) to determine how closely they approached the temperatures measured in the field at SZAL-2B and MAL-6.

Water temperatures were calculated using the average of all measured values of the  $\delta^{18}\text{O}_w$  of water and the  $\delta^{18}\text{O}_c$  of tufas. This was possible because there was no significant seasonal or downstream variation in  $\delta^{18}\text{O}_w$ . In the case of  $\delta^{18}\text{O}_c$ , the collected tufa at both studied sites precipitated during several (on average, 3–4) months. The calculated temperature data were compared with the measured water temperatures, although the latter was measured only when the carbonates were collected, once every 3–4 months. The measured  $\delta^{18}\text{O}_w$  can be used for temperature calculations for fossil tufas when the  $\delta^{18}\text{O}_w$  values are unknown. In such cases, the authors can infer that the  $\delta^{18}\text{O}$  of tufa precipitating from palaeo-water was the same as the  $\delta^{18}\text{O}_w$  of recent systems (Osácar et al. 2013).

We compared our estimated water temperature data from both study sites to the corrected mean annual air temperature ([www.ksh.hu](http://www.ksh.hu)<sup>1,2,3</sup>) and the measured spring temperatures, as the carbonate was deposited over several months and we only



had one water temperature value for the sampling date (Suppl. Table S4).

The correction for both sites was between the altitude of the meteorological stations and the altitude of the catchment area of the study site: 600–900 m, Bükk Plateau, Szalajka Valley and 200–400 m, Balaton Uplands, Malom Valley. The corrected mean annual air temperature requires a  $-0.5^{\circ}\text{C}/100\text{ m}$  correction, based on the altitude difference ( $1.6^{\circ}\text{C}$  and  $0.4^{\circ}\text{C}$  in the Szalajka and Malom Valleys, respectively).

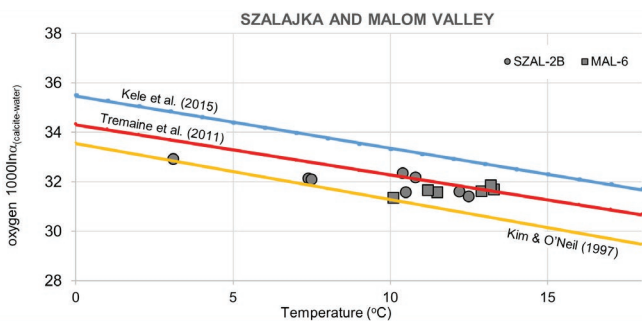


**Fig. 8.** The 1000lnα values of the SZAL-2B (Szalajka Valley) and MAL-6 (Malom Valley) samples, compared to water temperature and other published regression lines.

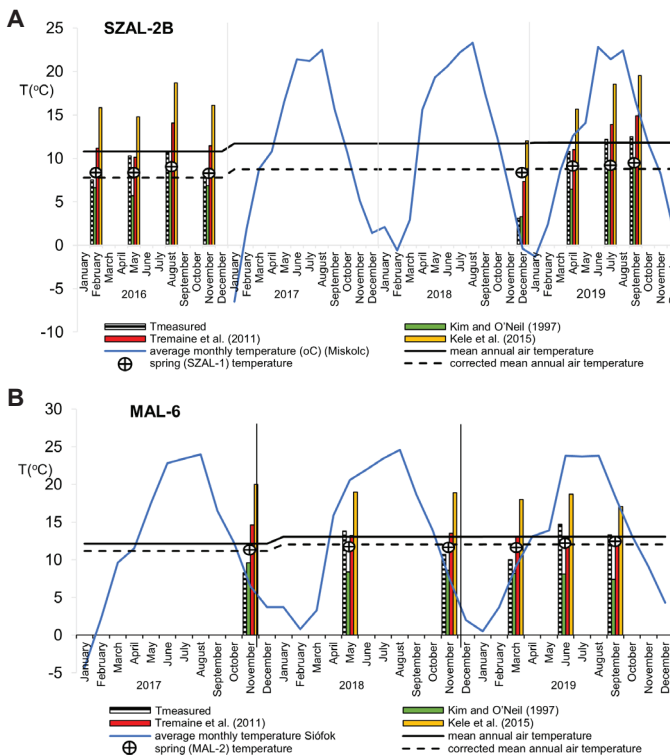


**Fig. 9. A** — Comparison of the mean annual air temperature, and the corrected mean annual air temperature with the calculated water temperature at the sampling point SZAL-2B (Szalajka Valley). **B** — Comparison of the mean annual air temperature with the calculated water temperature at the sampling point MAL-6 (Malom Valley).

Figures 9 A and B show that the spring’s water temperature is close to the corrected mean annual air temperature. The difference between them was less than or equal to  $1.3^{\circ}\text{C}$  in the Szalajka Valley and  $0.7^{\circ}\text{C}$  in the Malom Valley. Comparing the water temperatures calculated by the equation in Kim & O’Neil (1997) to the measured spring temperatures, the difference is within  $2.8^{\circ}\text{C}$  in the Szalajka Valley (1 exception: December of 2018,  $5.4^{\circ}\text{C}$ ) and  $4.7^{\circ}\text{C}$  in the Malom Valley. Using the equation of Tremaine et al. (2011), the difference between the calculated values and the spring temperature is  $\leq 5.5^{\circ}\text{C}$  in the Szalajka Valley and  $\leq 3.4^{\circ}\text{C}$  in the Malom Valley. In comparison to the corrected mean annual air temperature calculated with the Kim & O’Neil (1997) equation, the difference is  $\leq 2.3^{\circ}\text{C}$  in the Szalajka Valley (1 exception: December of 2018,  $5.4^{\circ}\text{C}$ ) and  $\leq 4.7^{\circ}\text{C}$  in the Malom Valley. The difference between the water temperature values calculated by the equation in Tremaine et al. (2011) and the corrected mean annual air temperature was within  $6.3^{\circ}\text{C}$  in the Szalajka Valley and  $3.5^{\circ}\text{C}$  in the Malom Valley. In both the Szalajka and Malom Valleys, the water temperature values calculated by the equation in Kele et al. (2015) show larger differences than the Kim & O’Neil (1997) and Tremaine et al. (2011) equations (relative to the spring temperature and corrected mean annual air temperature). A possible reason for this is that the Kele et al. (2015) equation is based primarily on travertine samples from a thermal spring measuring up to  $95^{\circ}\text{C}$ .

The difference between the mean annual air and spring water temperatures calculated by the equations in Kim & O’Neil (1997) and Tremaine et al. (2011) was  $\leq 1^{\circ}\text{C}$  for both study sites. The water temperature values calculated with the Tremaine et al. (2011) equation are closer to the measured water temperature at MAL-6 (Malom Valley) whereas the values calculated with the Kim & O’Neil (1997) equation are closer to the water temperature at SZAL-2B (Szalajka Valley). As such, the Kim & O’Neil (1997) equation can be applied for Szalajka Valley and the Tremaine et al. (2011) equation for Malom Valley. In conclusion, due to the effect of site-specific parameters, a single equation cannot be used to precisely calculate the deposition temperature of tufa carbonates at different research sites. In fact, our observations support the use of different, site-specific equations to accurately calculate the deposition temperature of tufa carbonates.

### Conclusions

Stable isotope composition study of recent fluvial tufa carbonates was carried out in the Szalajka Valley (Bükk Mts., Hungary) and Malom Valley (Balaton Uplands, Hungary) in order to find the most suitable places downstream for temperature calculation and to study the suitability of the published oxygen isotope-based palaeothermometers for tufa deposits.

- The stable oxygen isotope composition of both sites (the Szalajka and Malom Valley) stream waters were nearly constant downstream in all seasons. No seasonality was observed at both sites in the  $\delta^{18}\text{O}_w$  values. In the Malom Valley, no correlation was observed between  $\delta^{18}\text{O}_w$  and water temperature. Although the variation in the stable oxygen isotope composition of the Szalajka stream water was close to the uncertainty at each measurement point, it follows a similar pattern to the water temperature during the colder and warmer seasons. Since neither the  $\delta\text{D}$  nor  $\delta^{18}\text{O}_w$  changed, thus, the effect of evaporation is negligible.
- The  $\delta^{13}\text{C}_c$  and  $\delta^{18}\text{O}_c$  of the Szalajka and Malom tufa samples are similar to the data of tufas from the Bakony and Mecsek Mts., as well as to the values from neighbouring countries. The  $\delta^{18}\text{O}_c$  values of the studied Hungarian tufa are lower than those of Western Europe and higher than the  $\delta^{18}\text{O}_c$  values of tufa from countries east of Hungary (e.g., Belarus), confirming the increasing continentality from west to east, as described by Andrews (2006).
- In the Szalajka Valley, the best calculated temperatures were provided by the Kim & O'Neil (1997) equation, whereas in the Malom Valley, the Tremaine et al. (2011) equation provided the most precise temperatures.
- In both the Szalajka and Malom Valleys, we found a good correlation between  $1000\ln\alpha$  and the water temperatures close to the springs. This confirms the previous observations by Kele et al. (2008, 2011, 2015) about downstream travertine sections that the carbonates precipitating nearest to the spring orifice reflect close to equilibrium conditions. As such, they are the best places to collect tufas formed in the past and the most suitable for palaeotemperature calculation.
- Based on our observations, a single equation cannot be used for every study site to precisely calculate the deposition temperature of tufa carbonates. As a result, the use of different, site-specific equations is recommended.

**Acknowledgements:** This study was supported by the Talented Student Program of Eötvös Loránd University, Budapest and by the National Talent Programme (NTP-NFTÖ-18-B-0231) of the Ministry of Human Capacities. S.K. and B.B. received support from the KH 125584 project of the NKFIH (National Research, Development and Innovation Office, Hungary). This research was also supported by the European Union and the State of Hungary, co-financed by the European Regional Development Fund in the GINOP-2.3.2-15-2016-00009 'ICER' project. The authors wish to express their gratitude to Ariana Gugora for improving the English text.

## References

- Ambach W., Dansgaard W., Einser H. & Moller J. 1967: The altitude effect on the isotopic composition of precipitation and glacier ice in the Alps. *Tellus* 20, 596–600. <https://doi.org/10.3402/tellusa.v20i4.10040>
- Andrews J.E. 2006: Paleoclimatic records from stable isotopes in riverine tufas: Synthesis and review. *Elsevier, Earth–Science Reviews* 75, 85–104. <https://doi.org/10.1016/j.earscirev.2005.08.002>
- Andrews J.E. & Brasier A.T. 2005: Seasonal record of climatic change in annually laminated tufa: short review and future prospects. *Journal of Quaternary Science* 20, 411–421. <https://doi.org/10.1002/jqs.942>
- Aujeszky G. & Scheuer Gy. 1979: Hydrogeological experiences of the catchment of springs in W-Bükk Mts. *Hidrológiai Közlöny* 59, 63–77.
- Aujeszky G., Karácsonyi S. & Scheuer Gy. 1974: Karst hydrogeological conditions of SW Bükk Mts. *Hidrológiai Közlöny* 54, 465–476.
- Baráz Cs. (Ed.) 2002: The Bükk National Park: Mountains, forest, people. *Bükki Nemzeti Park Igazgatóság*, 1–621.
- Berrendero E., Arenas C., Mateo P. & Jones B. 2016: Cyanobacterial diversity and related sedimentary facies as a function of water flow conditions: Example from the Monasterio de Piedra Natural Park (Spain). *Sedimentary Geology* 337, 12–28. <https://doi.org/10.1016/j.sedgeo.2016.03.003>
- Bódai B., Kele S., Kármán K., Czuppon Gy. & Móga J. 2015: Stable isotope geochemical study of water and freshwater tufa of Csurgó spring (Bakony Mts., Hungary). *Karsztfejlődés* 20, 49–62 (in Hungarian with English abstract).
- Bódai B., Móga J., Bartha A., Holló S. & Kele S. 2016: Seasonal geochemical study of freshwater tufa of Szalajka creek (Bükk Mts., Hungary). *Karsztfejlődés* 21, 45–64 (in Hungarian with English abstract).
- Budai T., Császár G., Csillag G., Dudko A., Koloszar L. & Majoros Gy. 1999: Geology of the Balaton-felvidék. Explanatory to the geological map of the Balaton-felvidék. 1:50000. *Magyar Állami Földtani Intézet* 197, Alkalmi kiadványa, 1–310.
- Capezzuoli E., Gandin A. & Pedley M. 2014: Decoding tufa and travertine (fresh water carbonates) in the sedimentary record: The state of the art. *Sedimentology* 61, 1–21. <https://doi.org/10.1111/sed.12075>
- Czuppon Gy., Bottyán E., Krisztina K., Weidinger T. & Haszpra L. 2017: Significance of the air moisture source on the stable isotope composition of the precipitation in Hungary. In: *Proceedings of the Conference The EGU General Assembly 2017*, Vienna, Austria, 23–28 April 2017, 13458.
- Czuppon Gy., Demény A., Leél-Össy Sz., Óvári M., Molnár M., Stieber J., Kármán K., Kiss K. & Haszpra L. 2018: Cave monitoring in Béke and Baradla Caves (NE Hungary): implications for the condition of the formation of cave carbonates. *International Journal of Speleology* 47, 13–28.
- Dabkowski J. 2014: High potential of calcareous tufas for integrative multidisciplinary studies and prospects for archaeology in Europe. *Journal of Archaeological Science* 52, 72–83. <https://doi.org/10.1016/j.jas.2014.07.013>
- Dabkowski J., Brou L. & Naton H.G. 2015: New stratigraphic and geochemical data on the Holocene environment and climate from a tufa deposit at Direndall (Mamer Valley, Luxembourg). *The Holocene* 25, 1153–1164. <https://doi.org/10.1177/0959683615580183>
- Dabkowski J., Frodlová J., Hájek M., Hájková P., Petr L., Fiorillo D., Dudová L. & Horsák M. 2019: A complete Holocene climate and environment record for the Western Carpathians (Slovakia) derived from a tufa deposit. *The Holocene* 29, 493–504. <https://doi.org/10.1177/0959683618816443>
- Eiler J.M. 2007: Clumped-isotope geochemistry – the study of naturally-occurring, multiply-substituted isotopologues. *Earth and Planetary Science Letters* 262, 309–327. <https://doi.org/10.1016/j.epsl.2007.08.020>



- Epstein S., Buchsbaum R., Lowenstam H.A. & Urey H.C. 1951: Carbonate-water isotopic temperature scale. *Geological Society of America Bulletin* 62, 417–426. [https://doi.org/10.1130/0016-7606\(1951\)62\[417:CITS\]2.0.CO;2](https://doi.org/10.1130/0016-7606(1951)62[417:CITS]2.0.CO;2)
- Epstein S., Buchsbaum R., Lowenstam H.A. & Urey H.C. 1953: Revised carbonate-water isotopic temperature scale. *Geological Society of America Bulletin* 64, 1315–326. [https://doi.org/10.1130/0016-7606\(1953\)64\[1315:RCITS\]2.0.CO;2](https://doi.org/10.1130/0016-7606(1953)64[1315:RCITS]2.0.CO;2)
- Friedman I. & O'Neil J. R. 1977: Data of Geochemistry, Sixth Edition, Chapter KK. Compilation of Stable Isotope Fractionation Factors of Geochemical Interest. *Geological Survey Professional Paper* 440-KK, U. S. Government Printing Office, Washington. 1–12. <https://doi.org/10.3133/pp440KK>
- Garnett E.R., Andrews J.E., Preece R.C. & Dennis P.F. 2014: Climatic change recorded by stable isotopes and trace elements in a British Holocene tufa. *Journal of Quaternary Science* 3, 251–262. <https://doi.org/10.1002/jqs.842>
- Ghosh P., Adkins J., Affek H., Balta B., Guo W., Schauble E.A., Schrag D. & Eiler J.M. 2006:  $^{13}\text{C}$ – $^{18}\text{O}$  bonds in carbonate minerals: a new kind of paleothermometer. *Geochimica et Cosmochimica Acta* 70, 1439–1456. <https://doi.org/10.1016/j.gca.2005.11.014>
- Hevesi A. 1972: Freshwater carbonate formation in the Bükk Mts. *Földrajzi Értesítő* 21, 187–205 (in Hungarian).
- Hori M., Hoshino K., Okumura K. & Kano A. 2008: Seasonal patterns of carbon chemistry and isotopes in tufa depositing groundwaters of southwestern Japan. *Geochimica et Cosmochimica Acta* 72, 480–492. <https://doi.org/10.1016/j.gca.2007.10.025>
- Ihlenfeld C., Norman M.D., Gagan M.K., Drysdale R.N., Maas R. & Webb J. 2003: Climatic significance of seasonal trace element and stable isotope variations in a modern freshwater tufa. *Geochimica et Cosmochimica Acta* 67, 2341–2357. [https://doi.org/10.1016/S0016-7037\(02\)01344-3](https://doi.org/10.1016/S0016-7037(02)01344-3)
- Jenkins D.G. & Quintana-Ascencio P.F. 2020: A solution to minimum sample size for regressions. *PLoS ONE* 15, e0229345. <https://doi.org/10.1371/journal.pone.0229345>
- Kano A., Matsuoka J. & Fuji H. 2003: Origin of annual laminations in tufa deposits, southwest Japan. *Palaeogeography, Palaeoclimatology, Palaeoecology* 191, 243–262. [https://doi.org/10.1016/0031-0182\(02\)00717-4](https://doi.org/10.1016/0031-0182(02)00717-4)
- Kele S. 2009: Investigations on freshwater limestones from the Carpathian-Basin: paleoclimatological and sedimentological studies. *PhD Thesis, ELTE, Földtudományi Doktori Iskola*, 1–176.
- Kele S. & Bajnai D. 2017: Clumped isotopes in earth science research. *Földtani Közlemény* 147, 177–194. <https://doi.org/10.23928/foldt.kozl.2017.147.2.177>
- Kele S., Demény A., Silósy Z., Németh T., Tóth M. & Kovács B. M. 2008: Chemical and stable isotope composition of recent hot-water travertines and associated thermal waters, from Egerszalók, Hungary: Depositional facies and non-equilibrium fractionation. *Sedimentary Geology* 211, 53–72. <https://doi.org/10.1016/j.sedgeo.2008.08.004>
- Kele S., Özkül M., Fórizs I., Gökgöz A., Baykara O. M., Alçicek C. M. & Németh T. 2011: Stable isotope geochemical study of Pamukkale travertines: New evidence of low-temperature non-equilibrium calcite-water fractionation. *Sedimentary Geology* 238, 191–212. <https://doi.org/10.1016/j.sedgeo.2011.04.015>
- Kele S., Breitenbach S. F. M., Capezzuoli E., Meckler A. N., Ziegler M., Millan I. M., Kluge T., Deák J., Hanselmann K., John C. M., Yan H., Liu Z. & Bernasconi S. M. 2015: Temperature dependence of oxygen- and clumped isotope fractionation in carbonates: A study of travertines and tufas in the 6–95 °C temperature range. *Geochimica et Cosmochimica Acta* 168, 172–192. <https://doi.org/10.1016/j.gca.2015.06.032>
- Kern Z., Hatvani I.G., Czuppon Gy., Fórizs I., Erdélyi D., Kanduč T., Palcsu L. & Vreča P. 2020: Isotopic ‘altitude’ effect and ‘continental’ effect in modern precipitation across the Adriatic–Pannonian region. *Water* 12, 1797. <https://doi.org/10.3390/w12061797>
- Kim S.T. & O'Neil J.R. 1997: Equilibrium and nonequilibrium oxygen isotope effects in synthetic carbonates. *Geochimica et Cosmochimica Acta* 61, 3461–3475. [https://doi.org/10.1016/S0016-7037\(97\)00169-5](https://doi.org/10.1016/S0016-7037(97)00169-5)
- Koltai G., Kele S. & Keveiné B.I. 2012b: Preliminary studies of freshwater tufa deposits in Mecsek Mts., Hungary. *Acta Climatologica et Chorologica, Universitas Szegediensis* 46, 143–151.
- Koltai G., Kele S., Kármán K. & Keveiné B.I. 2012a: Geochemical study of freshwater tufa deposits in the Mecsek Mts.. *Karsztfejlődés XVII. Szombathely*, 35–46.
- Lojen S., Dolenc T., Vokal B., Cukrov N., Mihelcic G. & Papesch W. 2004: C and O stable isotope variability in recent freshwater carbonates (River Krka, Croatia). *Sedimentology* 51, 361–375. <https://doi.org/10.1111/j.1365-3091.2004.00630.x>
- Lojen S., Trkov A., Scancar J., Vázquez-Navarro J. A. & Cukrov N. 2009: Continuous 60-year stable isotopic and earth-alkali element records in a modern laminated tufa (Jaruga, river Krka, Croatia): Implications for climate reconstruction. *Chemical Geology* 258, 242–250. <https://doi.org/10.1016/j.chemgeo.2008.10.013>
- Matsuoka J., Kano A., Oba T., Watanabe T., Sakai S. & Seto K. 2001: Seasonal variation of stable isotopic compositions recorded in a laminated tufa, SW Japan. *Earth and Planetary Science Letters* 192, 31–44. [https://doi.org/10.1016/S0012-821X\(01\)00435-6](https://doi.org/10.1016/S0012-821X(01)00435-6)
- McCrea J.M. 1950: On the Isotopic Chemistry of Carbonates and a Paleotemperature Scale. *The Journal of Chemical Physics* 18, 849–857. <https://doi.org/10.1063/1.1747785>
- Országos Meteorológiai Szolgálat (OMSZ) 2001: Climate atlas of Hungary. *Országos Meteorológiai Szolgálat*, 1–108.
- Osácar M.C., Arenas C., Vaquez-Urbez M., Sancho C. & Auqué L.F. 2013: Environmental factors controlling the  $\delta^{13}\text{C}$  and  $\delta^{18}\text{O}$  variations of recent fluvial tufas: a 12-year record from the Monasterio De Piedra Natural Park (Ne Iberian Peninsula). *Journal of Sedimentary Research* 83, 309–322. <https://doi.org/10.2110/jsr.2013.27>
- Paul D., Skrzypek G. & Fórizs I. 2007: Normalization of measured stable isotopic compositions to isotope reference scales – a review. *Rapid Communications in Mass Spectrometry* 21, 3006–3014. <https://doi.org/10.1002/rcm.3185>
- Pazdur A. 1988: The relations between carbon isotope composition and apparent age of freshwater tuffaceous sediments. *Radio-carbon* 30, 1–18. <https://doi.org/10.1017/S0033822200043915>
- Pelikán P. (Ed.) 2005: Geology of the Bükk Mountains. *Magyar Állami Földtani Intézet*, Budapest, 1–284.
- Pentecost A. 2005: Travertine. *Springer-Verlag*, 1–445.
- Spötl C. & Vennemann T.W. 2003: Continuous-flow isotope ratio mass spectrometric analysis of carbonate minerals. *Rapid communications in mass spectrometry* 17, 1004–1006. <https://doi.org/10.1002/rcm.1010>
- Tremaine D.M., Froelich P.N. & Wang Y. 2011: Speleothem calcite farmed in situ: modern calibration of  $\delta^{18}\text{O}$  and  $\delta^{13}\text{C}$  paleoclimate proxies in a continuously-monitored natural cave system. *Geochimica et Cosmochimica Acta* 75, 4929–4950. <https://doi.org/10.1016/j.gca.2011.06.005>

- Urey H. C. 1947: The thermodynamic properties of isotopic substances. *Journal of the Chemical Society*, 562–581. <https://doi.org/10.1039/jr9470000562>
- www.ksh.hu<sup>1</sup>: [https://www.ksh.hu/stadat\\_files/kor/ku/kor0075.html](https://www.ksh.hu/stadat_files/kor/ku/kor0075.html) (accessed 2022.03.25)
- www.ksh.hu<sup>2</sup>: [https://www.ksh.hu/docs/hun/xstadat/xstadat\\_evkozi/e\\_met007.html](https://www.ksh.hu/docs/hun/xstadat/xstadat_evkozi/e_met007.html) (accessed 2022.03.25)
- www.ksh.hu<sup>3</sup>: [https://www.ksh.hu/docs/hun/xstadat/xstadat\\_eves/i\\_met002cc.html](https://www.ksh.hu/docs/hun/xstadat/xstadat_eves/i_met002cc.html) (accessed 2022.03.25)
- www.bnpi.hu: <https://www.bnpi.hu/hu/reszletek/szalajka-forras> (accessed 2022.03.25)
- www.map.mbfisz.gov.hu: [https://map.mbfisz.gov.hu/fdt\\_alapszelvenyek/](https://map.mbfisz.gov.hu/fdt_alapszelvenyek/) (accessed 2022.03.25)
- Zsilák Gy.L. 1960: Hydrological and hydrogeological study of the Szalajka Valley (Szilvásvár, Hungary). *Hidrológiai Közöny* 1, 58–64 (in Hungarian).

**Electronic supplementary material** is available online:

Suppl. Table S1 at [http://geologicacarpatica.com/data/files/GC-73-5-Bodai\\_TableS1.docx](http://geologicacarpatica.com/data/files/GC-73-5-Bodai_TableS1.docx)

Suppl. Table S2 at [http://geologicacarpatica.com/data/files/GC-73-5-Bodai\\_TableS2.docx](http://geologicacarpatica.com/data/files/GC-73-5-Bodai_TableS2.docx)

Suppl. Table S3 at [http://geologicacarpatica.com/data/files/GC-73-5-Bodai\\_TableS3.docx](http://geologicacarpatica.com/data/files/GC-73-5-Bodai_TableS3.docx)

Suppl. Table S4 at [http://geologicacarpatica.com/data/files/GC-73-5-Bodai\\_TableS4.docx](http://geologicacarpatica.com/data/files/GC-73-5-Bodai_TableS4.docx)



## Supplement

**Table S1:** *In situ*, seasonally measured parameters and stable isotopic compositions of water and tufa in the Szalajka Valley. The empty cells show that the plastic surface used for carbonate collection was not detected or that there was no carbonate on it.

Date	Code	T (°C)	pH	EC ( $\mu\text{S}/\text{cm}$ )	$\delta^{18}\text{O}_w$ (‰, V-SMOW)	$\delta\text{D}_w$ (‰, V-SMOW)	$\delta^{13}\text{C}_c$ (‰, V-PDB)	$\delta^{18}\text{O}_c$ (‰, V-PDB)	$\delta^{18}\text{O}_c$ (‰, V-SMOW)
11.02.2016.	SZAL-1	8.9	7.27	490	-10.5	-71			
	SZAL-2A	7.5	7.91	480					
	SZAL-2B	7.4	7.93	480	-10.6	-71	-9.8	-8.7	21.9
	SZAL-2C	7.5	8.24	470	-10.6	-72	-9.9	-8.0	22.7
	SZAL-3	7.4	8.29	400	-10.6	-72	-10.1	-8.5	22.1
	SZAL-4	8.1	8.16	460	-10.4	-70	-9.9	-8.6	22.0
	SZAL-5	8.5	8.13	390	-10.4	-71	-9.4	-8.7	22.0
SZAL-6	7.0	8.35	400	-10.5	-72	-9.4	-9.4	21.3	
22.05.2016.	SZAL-1	8.5	7.82	486	-10.5	-70			
	SZAL-2A	10.3	8.20	488					
	SZAL-2B	10.4	8.28	484	-10.5	-70	-9.8	-8.5	22.1
	SZAL-2C	10.7	8.92	470	-10.5	-70	-9.8	-8.5	22.2
	SZAL-3	10.9	8.31	458	-10.5	-69	-9.9	-8.3	22.4
	SZAL-4	11.4	8.03		-10.4	-70	-9.7	-8.6	22.0
	SZAL-5	11.4	8.71		-10.3	-70	-9.0	-8.7	21.9
SZAL-6	12.0	8.48		-10.1	-69	-9.4	-9.0	21.7	
16.08.2016.	SZAL-1	9.1	7.21	464	-10.4	-72			
	SZAL-2A	10.8	8.07	468					
	SZAL-2B	10.5	8.52	476	-10.3	-70	-10.5	-9.3	21.3
	SZAL-2C	10.9	8.85	454	-10.3	-70	-10.2	-8.9	21.7
	SZAL-3	11.3	8.55	450	-10.3	-70	-9.4	-8.5	22.2
	SZAL-4	12.6	7.89	412	-10.2	-70	-10.1	-8.6	22.0
	SZAL-5	12.6	8.22	448	-10.2	-70	-10.0	-8.8	21.8
SZAL-6	15.3	8.07	444	-10.0	-70	-9.3	-8.8	21.8	
12.11.2016.	SZAL-1	8.7	7.66	478	-10.4	-71			
	SZAL-2A	7.7	8.23	478					
	SZAL-2B	7.5	8.26	466	-10.3	-71	-10.3	-8.8	21.9
	SZAL-2C	7.5	8.88	470	-10.4	-71	-10.0	-9.0	21.6
	SZAL-3	7.8	8.74	448	-10.4	-71	-10.0	-8.5	22.2
	SZAL-4	8.6	8.53	474	-10.3	-70	-10.2	-8.5	22.1
	SZAL-5	8.9	8.85	398	-10.3	-70	-9.9	-8.6	22.0
SZAL-6	7.5	8.84	478	-10.0	-69	-9.8	-8.8	21.8	
15.12.2018.	SZAL-1	8.7	7.47	486	-10.5	-71			
	SZAL-2A	3.2	8.37	477	-10.5	-71	-10.2	-8.6	22.1
	SZAL-2B	3.1	8.77	474	-10.5	-72	-9.1	-7.9	22.7
	SZAL-2C	2.8	8.38	458	-10.5	-72			
	SZAL-3	1.4	8.46	447	-10.6	-72			
	SZAL-4	9.0	8.16	470	-10.4	-71			
	SZAL-5	8.8	8.59	468	-10.4	-71	-8.9	-9.8	20.8
SZAL-6	4.6	8.59	474	-10.3	-71	-9.9	-9.0	21.6	
20.04.2019.	SZAL-1	8.9	6.47	481	-10.6	-72			
	SZAL-2A	11.4	8.37	458	-10.4	-71	-9.2	-8.8	21.8
	SZAL-2B	10.8	8.10	450	-10.3	-70	-9.5	-8.7	22.0
	SZAL-2C	11.0	8.55	438	-10.3	-71	-10.0	-8.0	22.7
	SZAL-3	9.8	8.30	424	-10.3	-70			
	SZAL-4	10.4	8.11	465	-10.4	-71			
	SZAL-5	10.5	8.30	464	-10.4	-71			
SZAL-6	11.5	8.57	443	-10.1	-70	-7.9	-8.4	22.3	
09.07.2019.	SZAL-1	9.0	7.41	494	-10.4	-71			
	SZAL-2A	12.2	7.91	479	-10.3	-71	-10.4	-9.1	21.5
	SZAL-2B	12.2	8.02	456	-10.3	-71	-10.8	-9.2	21.4
	SZAL-2C	12.3	8.05	458	-10.3	-71	-10.6	-9.1	21.6
	SZAL-3	12.3	7.99	447	-10.3	-70			
	SZAL-4	12.2	7.94	460	-10.5	-70			
	SZAL-5	12.2	8.08	462	-10.4	-70			
SZAL-6	14.5	8.20	443	-10.3	-70	-10.2	-9.8	20.8	
25.09.2019.	SZAL-1	9.4	7.44	485	-10.5	-71			
	SZAL-2A	12.5	8.03	432	-10.3	-71	-9.9	-9.2	21.4
	SZAL-2B	12.5	8.06	458	-10.4	-71	-10.0	-9.4	21.2
	SZAL-2C	12.7	8.13	443	-10.3	-70	-9.7	-9.2	21.5
	SZAL-3	15.4	8.01	410	-10.2	-70	-9.6	-8.8	21.9
	SZAL-4	12.8	7.79	497	-10.4	-71	-8.3	-8.8	21.9
	SZAL-5	12.9	8.01	499	-10.4	-71	-10.0	-9.2	21.4
SZAL-6	13.8	8.16	477	-10.2	-70	-10.2	-10.1	20.5	

**Table S2:** *In situ*, seasonally measured parameters and stable isotopic composition of water and tufa in the Malom Valley. The empty cells show that the plastic surface used for carbonate collection was not detected or that there was no carbonate on it.

Date	Code	T (°C)	pH	EC ( $\mu\text{S/cm}$ )	$\delta^{18}\text{Ow}$ (‰, V-SMOW)	$\delta\text{Dw}$ (‰, V-SMOW)	$\delta^{13}\text{Cc}$ (‰, V-PDB)	$\delta^{18}\text{Oc}$ (‰, V-PDB)	$\delta^{18}\text{Oe}$ (‰, V-SMOW)	
25.11.2017.	MAL-1	11.2	7.34	496	-9.6	-70				
	MAL-2	11.2	7.34	496	-9.6	-70				
	MAL-3	10.9	7.64	906						
	MAL-5	10.5	8.20	906	-9.6	-68	-9.8	-8.3	22.4	
	MAL-6	10.1	8.43	892	-9.6	-70	-10.5	-8.7	21.9	
	MAL-7	9.8	8.48	887	-9.7	-69	-10.0	-8.4	22.2	
	MAL-8	9.4	8.47	886	-9.6	-68	-9.9	-8.6	22.0	
	MAL-10	9.0	8.41	884	-9.5	-70	-10.0	-8.6	22.1	
	MAL-12	8.7	8.37	833	-9.6	-69	-10.0	-8.5	22.1	
	MAL-13	8.7	8.41	875	-9.6	-68	-9.7	-8.7	22.0	
	MAL-14	8.5	8.42	864	-9.7	-68	-9.9	-8.7	21.9	
	MAL-15	8.3	8.37	862	-9.8	-68	-9.1	-8.2	22.4	
	30.05.2018.	MAL-1	11.8	7.15	868	-9.6	-69			
		MAL-2	11.7	7.22	837	-9.7	-69			
		MAL-3	12.0	7.43	851	-9.7	-68			
MAL-5		12.5	7.92	856	-9.7	-68	-9.1	-8.3	22.3	
MAL-6		12.9	8.11	852	-9.5	-68	-9.9	-8.5	22.2	
MAL-7		13.7	8.16	847	-9.7	-68	-10.0	-8.4	22.3	
MAL-8		13.4	7.97	841	-9.7	-68	-10.3	-8.4	22.3	
MAL-10		13.4	8.24	835	-9.6	-68	-10.4	-8.7	22.0	
MAL-12		13.7	8.27	813	-9.7	-68	-10.1	-8.5	22.1	
MAL-13		13.8	8.25	813	-9.6	-68	-9.9	-8.4	22.3	
MAL-14		13.9	8.32	810	-9.5	-68	-9.9	-8.5	22.1	
MAL-15		13.8	8.08	801	-9.7	-68	-9.9	-8.5	22.1	
06.10.2018.		MAL-1	11.8	7.35	857	-9.7	-68			
		MAL-2	11.8	7.13	841	-9.8	-68			
		MAL-3	11.8	7.38	835	-9.7	-68			
	MAL-5	11.4	8.51	790	-9.6	-68	-9.2	-8.0	22.7	
	MAL-6	11.5	8.05	845	-9.6	-68	-10.1	-8.5	22.1	
	MAL-7	11.6	8.26	837	-9.7	-68	-10.4	-8.7	21.9	
	MAL-8	11.6	8.33	834	-9.8	-68	-10.2	-8.6	22.1	
	MAL-10	11.5	8.35	830	-9.7	-68	-10.1	-8.5	22.1	
	MAL-12	11.3	8.28	814	-9.5	-68	-10.5	-8.8	21.8	
	MAL-13	11.1	8.44	817	-9.7	-68	-10.3	-9.0	21.7	
	MAL-14	10.7	8.47	809	-9.7	-68	-10.3	-8.9	21.7	
	MAL-15	10.7	8.47	801	-9.8	-68	-9.8	-8.6	22.0	
	09.03.2019.	MAL-1	10.7	7.75	855	-9.6	-68			
		MAL-2	11.3	7.38	832	-9.7	-69			
		MAL-3	11.2	7.46	838	-9.6	-69			
MAL-5		11.1	8.18	846	-9.7	-68	-10.3	-8.3	22.3	
MAL-6		11.2	8.35	837	-9.7	-68	-10.5	-8.4	22.2	
MAL-7		10.9	8.40	827	-9.4	-68	-10.5	-8.4	22.2	
MAL-8		10.5	8.39	820	-9.5	-68	-10.3	-8.3	22.4	
MAL-10		10.5	8.47	820	-9.5	-67	-10.2	-8.3	22.3	
MAL-12		10.3	8.51	806	-9.7	-68	-9.9	-8.0	22.7	
MAL-13		10.6	8.56	802	-9.4	-68				
MAL-14		10.1	8.54	789	-9.6	-68	-9.8	-8.0	22.6	
MAL-15		10.0	8.60	787	-9.5	-68	-9.9	-8.1	22.5	
22.06.2019.		MAL-1	12.8	7.59	867	-9.7	-69			
		MAL-2	12.2	7.34	843	-9.6	-69			
		MAL-3	12.0	7.28	838	-9.6	-68			
	MAL-5	13.1	7.94	845	-9.6	-68				
	MAL-6	13.3	8.15	836	-9.5	-67	-10.3	-8.4	22.2	
	MAL-7	14.1	8.16	826	-9.6	-68	-10.4	-8.8	21.9	
	MAL-8	14.2	8.20	820	-9.7	-68				
	MAL-10	14.4	8.22	816	-9.5	-68	-10.3	-8.8	21.9	
	MAL-12	14.6	8.23	807	-9.6	-68				
	MAL-13	14.7	8.21	784	-9.7	-67	-10.1	-8.8	21.8	
	MAL-14									
	MAL-15	14.7	8.25	775	-9.6	-68	-9.9	-8.9	21.8	
	13.09.2019.	MAL-1	12.6	7.62	851	-9.7	-69			
		MAL-2	12.3	7.49	837	-9.8	-69			
		MAL-3	12.2	7.41	839	-9.9	-68			
MAL-5		12.8	8.10	816	-9.8	-68	-10.2	-8.3	22.4	
MAL-6		13.2	8.24	831	-9.7	-68	-10.2	-8.2	22.4	
MAL-7		13.5	8.20	822	-9.7	-68	-10.0	-8.4	22.2	
MAL-8		13.4	8.23	812	-9.5	-68	-9.8	-8.5	22.1	
MAL-10		13.3	8.30	810	-9.6	-68				
MAL-12		13.4	8.36	792	-9.7	-69	-9.6	-8.4	22.2	
MAL-13		13.1	8.38	789	-9.7	-69	-9.9	-8.9	21.7	
MAL-14		13.3	8.41	777	-9.6	-68	-9.5	-8.5	22.2	
MAL-15		13.3	8.42	776	-9.7	-68	-9.7	-9.0	21.6	

**Table S3:** The correlation between the  $1000\ln\alpha$  values and temperature at selected sampling points in the Szalajka and Malom Valleys.

Date	Code	T (°C)	$1000\ln\alpha$	r	p value	No. of samples
15.12.2018 20.04.2019 09.07.2019 25.09.2019	SZAL-2A	3.2	32.17	<b>0.8541</b>	<b>0.1459</b>	<b>4</b>
		11.4	31.93			
		12.2	31.62			
		12.5	31.48			
11.02.2016 22.05.2016 16.08.2016 12.11.2016 15.12.2018 20.04.2019 09.07.2019 25.09.2019	SZAL-2B	7.4	32.02	<b>0.8329</b>	<b>0.0102</b>	<b>8</b>
		10.4	32.23			
		10.5	31.45			
		7.5	31.97			
		3.1	32.80			
		10.8	32.06			
		12.2	31.49			
		12.5	31.29			
11.02.2016 22.05.2016 16.08.2016 12.11.2016 20.04.2019 09.07.2019 25.09.2019	SZAL-2C	7.5	32.73	<b>0.3693</b>	<b>0.4150</b>	<b>7</b>
		10.7	32.26			
		10.9	31.80			
		7.5	31.70			
		11	32.79			
		12.3	31.66			
		12.7	31.57			
11.02.2016 22.05.2016 16.08.2016 12.11.2016 09.07.2019 25.09.2019	SZAL-3	7.4	32.19	<b>0.2486</b>	<b>0.6347</b>	<b>6</b>
		10.9	32.44			
		11.3	32.25			
		7.8	32.28			
		12.3	10.33			
		15.4	31.95			
25.11.2017 30.05.2018 06.10.2018 09.03.2019 13.09.2019	MAL-5	10.5	31.81	<b>0.1650</b>	<b>0.7911</b>	<b>5</b>
		12.5	31.78			
		11.4	32.09			
		11.1	31.78			
		12.8	31.80			
25.11.2017 30.05.2018 06.10.2018 09.03.2019 22.06.2019 13.09.2019	MAL-6	10.1	31.36	<b>0.8147</b>	<b>0.0483</b>	<b>6</b>
		12.9	31.62			
		11.5	31.57			
		11.2	31.66			
		13.3	31.68			
		13.2	31.86			
25.11.2017 30.05.2018 06.10.2018 09.03.2019 22.06.2019 13.09.2019	MAL-7	9.8	31.64	<b>0.2133</b>	<b>0.6845</b>	<b>6</b>
		13.7	31.70			
		11.6	31.39			
		10.9	31.67			
		14.1	31.33			
		13.5	31.67			
25.11.2017 30.05.2018 06.10.2018 09.03.2019 13.09.2019	MAL-8	9.4	31.44	<b>0.3039</b>	<b>0.6191</b>	<b>5</b>
		13.4	31.71			
		11.6	31.49			
		10.5	31.80			
		13.4	31.59			
25.11.2017 30.05.2018 06.10.2018 09.03.2019 22.06.2019	MAL-10	9	31.50	<b>0.6592</b>	<b>0.2262</b>	<b>5</b>
		13.4	31.43			
		11.5	31.59			
		10.5	31.76			
		14.40	31.30			
25.11.2017 30.05.2018 06.10.2018 09.03.2019 13.09.2019	MAL-12	8.7	31.61	<b>0.2536</b>	<b>0.6806</b>	<b>5</b>
		13.7	31.48			
		11.3	31.27			
		10.3	32.05			
		13.4	31.68			
25.11.2017 30.05.2018 06.10.2018 22.06.2019 13.09.2019	MAL-13	8.7	31.40	<b>0.1043</b>	<b>0.8675</b>	<b>5</b>
		13.8	31.71			
		11.1	31.10			
		14.7	31.25			
		13.1	31.16			
25.11.2017 30.05.2018 06.10.2018 09.03.2019 13.09.2019	MAL-14	8.5	31.35	<b>0.1206</b>	<b>0.8468</b>	<b>5</b>
		13.9	31.57			
		10.7	31.17			
		10.1	32.06			
		13.3	31.62			
25.11.2017 30.05.2018 06.10.2018 09.03.2019 22.06.2019 13.09.2019	MAL-15	8.3	31.84	<b>0.7710</b>	<b>0.0727</b>	<b>6</b>
		13.8	31.57			
		10.7	31.47			
		10	31.98			
		14.7	31.21			
		13.3	31.09			



**Table S4:** Summary table of the calculated and measured water temperature values and their difference in the Szalajka and Malom Valleys. The numbers 1, 2 and 3 indicate the equations used, see above.

Date	Code	Kim and O'Neil (1997) <sup>1</sup>	$T_{spring}^{water}$	$T_{c.m.a}^{air}$	Tremaine et al. (2011) <sup>2</sup>	$T_{spring}^{water}$	$T_{c.m.a}^{air}$	Kele et al. (2015) <sup>3</sup>	$T_{spring}^{water}$	$T_{c.m.a}^{air}$	T <sub>measured</sub>	mean annual air T (Miskolc/Siófok)	corrected mean annual air T (Miskolc/Siófok)
			– $T_{calc}^1$	– $T_{calc}^1$		– $T_{calc}^2$	– $T_{calc}^2$		– $T_{calc}^3$	– $T_{calc}^3$			
(°C)													
11.02.2016	spring(SZAL-1) SZAL-2B	6.6	2.3	1.2	11.2	-2.3	-3.4	15.8	-6.9	-8.0	8.9 7.4	10.8 10.8	7.8 7.8
22.05.2016	spring(SZAL-1) SZAL-2B	5.7	2.8	2.1	10.1	-1.6	-2.3	14.8	-6.3	-7.0	8.5 10.4	10.8 10.8	7.8 7.8
16.08.2016	spring(SZAL-1) SZAL-2B	9.1	0.0	-1.3	14.1	-5.0	-6.3	18.7	-9.6	-10.9	9.1 10.5	10.8 10.8	7.8 7.8
12.11.2016	spring(SZAL-1) SZAL-2B	6.9	1.8	0.9	11.5	-2.8	-3.7	16.1	-7.4	-8.3	8.7 7.5	10.8 10.8	7.8 7.8
15.12.2018	spring(SZAL-1) SZAL-2B	3.3	5.4	5.4	7.3	1.4	1.4	12.0	-3.3	-3.3	8.7 3.1	11.7 11.7	8.7 8.7
20.04.2019	spring(SZAL-1) SZAL-2B	6.5	2.4	2.3	11.0	-2.1	-2.2	15.7	-6.8	-6.9	8.9 10.8	11.7 11.8	8.7 8.8
09.07.2019	spring(SZAL-1) SZAL-2B	9.0	0.0	-0.2	13.9	-4.9	-5.1	18.5	-9.5	-9.7	9.0 12.2	11.8 11.8	8.8 8.8
25.09.2019	spring(SZAL-1) SZAL-2B	9.8	-0.4	-1.0	14.9	-5.5	-6.1	19.5	-10.1	-10.7	9.4 12.5	11.8 11.8	8.8 8.8
25.11.2017	spring(MAL-2) MAL-6	9.6	1.6	1.5	14.6	-3.4	-3.5	20.0	-8.8	-8.9	11.2 8.3	12.1 12.1	11.1 11.1
30.05.2018	spring(MAL-2) MAL-6	8.4	3.3	3.6	13.2	-1.5	-1.2	19.0	-7.3	-7.0	11.7 13.8	13.0 13.0	12.0 12.0
06.10.2018	spring(MAL-2) MAL-6	8.6	3.2	3.4	13.5	-1.7	-1.5	18.9	-7.1	-6.9	11.8 10.7	13.0 13.0	12.0 12.0
09.03.2019	spring(MAL-2) MAL-6	8.2	3.1	3.9	13.1	-1.8	-1.0	18.0	-6.7	-5.9	11.3 10.0	13.0 13.1	12.0 12.1
22.06.2019	spring(MAL-2) MAL-6	8.1	4.1	4.0	12.9	-0.7	-0.8	18.7	-6.5	-6.6	12.2 14.7	13.1 13.1	12.1 12.1
13.09.2019	spring(MAL-2) MAL-6	7.4	4.9	4.7	12.0	0.3	0.1	17.1	-4.8	-5.0	12.3 13.3	13.1 13.1	12.1 12.1